1. Introduction

<INN> drug substance is a synthetic molecule and isolated as a <anhydrous crystalline solid, hydrochloride salt, etc>.

Figure 1. Structural Formula of <INN>

<insert figure>

2. Elucidation of Structure

Confirmation of the chemical structure of <INN> is provided by <elemental analysis, Nuclear Magnetic Resonance (NMR) spectroscopy, Mass spectrometry (MS), Ultraviolet/visible (UV/Vis) absorption, Fourier Transform Infrared (FTIR) absorption spectroscopy, and Single Crystal X-ray diffraction>. Characterization studies were performed using Primary Reference standard lot XXXXXXXXXX which was derived from drug substance lot XXXXXXXXXX, unless otherwise noted. The characterization data of <INN> drug substance supports the chemical structure assigned. The preparation of the standard is described in 3.2.S.5 (Reference Standards or Materials).

2.1 Elemental Analysis

The elemental analysis results provided below are consistent with the theoretical composition of <INN>.

Table 1. Elemental Analysis of <INN>

Element	Theoretical (%)	Results (%)
C	XX.XX	XX.XX
H	X.XX	X.XX
N	X.XX	X.XX
F	X.XX	X.XX

2.2 Mass Spectrometry

Accurate mass measurements supported the <INN> molecular formula ($C_{XX}H_{XX}N_{XX}F_{XX}O_{XX}$). The mass spectrum was obtained by a single mass scan on an electrostatic orbital ion trap Fourier Transform Mass Spectrometer (FTMS) using external calibration with sample introduction via Electrospray Ionization (ESI). The theoretical exact masses for the singly, doubly and triply charged molecular ions, $[M+H]^{+}$, $[M+2H]^{2+}$ and $[M+3H]^{3+}$, of <INN> are XXX.XXXXX Daltons, XXX.XXXXX Daltons and XXX.XXXXX Daltons, respectively. The mass spectrum of primary reference standard lot XXXXXX (Figure 2) exhibits a singly charged molecular ion at the m/z value of

XXX.XXXXX Daltons (mass accuracy: X.XX ppm), doubly charged molecular ion at the m/z value of XXX.XXXXX Daltons (mass accuracy: X.XX ppm) and triply charged molecular ion at XXX.XXXXX Daltons (mass accuracy: X.XX ppm), consistent with the molecular formula ($C_{XX}H_{XX}N_{XX}F_{XX}O_{XX}$). Furthermore, the higher-energy collisional dissociation (HCD)-MS/MS mass spectrum of the triply charged molecular ion (Figure 3) reflects a fragmentation pattern (Figure 4) that is consistent with the assigned structure of <INN>. Table 2 summarizes the observed fragment ions.

Figure 2. ESI Mass Spectrum of <INN> (Lot XXXXXXXXXX)

<insert figure>

Figure 3. HCD-MS/MS Mass Spectrum of <INN> (Lot XXXXXXXXXX)

<insert figure>

Figure 4. Interpretation of HCD-MS/MS Fragmentation of <INN> (Lot XXXXXXXXXX)

<insert figure>

Table 2. List of Theoretical and Observed HCD-MS/MS Ions for <INN> (Lot XXXXXXXXXX)

Theoretical m/z	Observed m/z	Mass Accuracy ppm Difference
XXX.XXXXX	XXX.XXXXX	+/- X.XXX
XXX.XXXXX	XXX.XXXXX	+/- X.XXX
XXX.XXXXX	XXX.XXXXX	+/- X.XXX
XXX.XXXXX	XXX.XXXXX	+/- X.XXX

2.3 Proton (^{1}H) and Carbon (^{13}C) Nuclear Magnetic Resonance (NMR) Spectroscopy

The analyses of ^{1}H, ^{13}C, ^{15}N, and ^{19}F NMR data support the assigned structure of <INN>. 1D and 2D spectra were recorded in DMSO (DMSO-d_6) at 27°C (300 K). NMR spectra were acquired at XXX.XX MHz for ^{1}H, XXX.XX MHz for ^{13}C, and XXX.XX MHz for ^{15}N, and XXX.XX for ^{19}F on the spectrometer. Data processing was carried out using the spectrometer software. Chemical shifts are reported in the δ scale (ppm) by assigning the residual solvent peak to X.XX ppm for CD_2HSOCD_3 for ^{1}H, XX.XX ppm for the methyl group of DMSO for ^{13}C (default on the spectrometer setup), X.XX ppm for liquid NH_3 for ^{15}N (default on the spectrometer setup), and 0.00 ppm for liquid $CFCl_3$ for ^{19}F (default on the spectrometer setup).

The 1D ^{1}H and ^{13}C NMR spectra of <INN> are shown in Figure 5 and Figure 6, respectively. The chemical shift assignments presented in Table 3 refer to the numbered structure of <INN> shown in Figure 7.

Figure 5. ^{1}H NMR Spectrum of <INN> (Lot XXXXXXXXXX) in DMSO-d_6

<insert figure>

Figure 6. ^{13}C NMR Spectrum of <INN> (Lot XXXXXXXXXX) in DMSO-d_6

<insert figure>

Figure 7. Structure of <INN> With Number Assignments

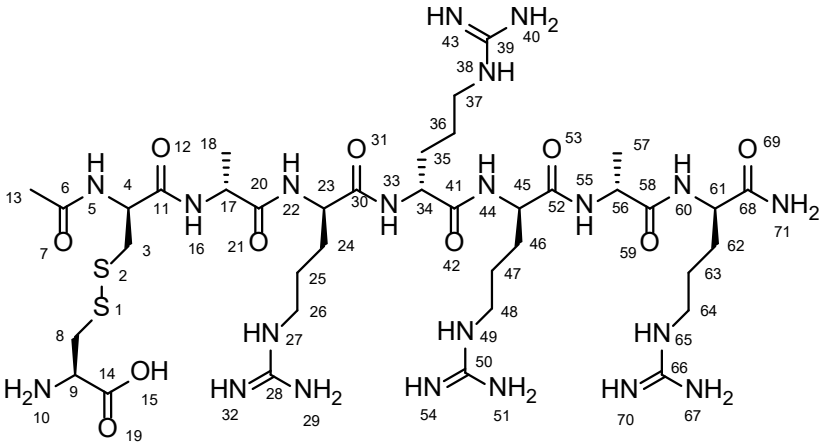

Table 3. Interpretation of the 1D ^{1}H NMR and ^{13}C NMR Spectra of <INN> (Lot XXXXXXXXXX) in DMSO-d_6

Position[a]	^{1}H (δ/ppm, J/Hz)[b,c]	^{13}C (δ/ppm)[b,c]
3	2.903 (dd, J=13.5, 9.6 Hz, 1H), 3.174 (dd, J=13.5, 4.4 Hz, 1H)	40.35
4	4.558 (ddd, J=9.6, 8.0, 4.4 Hz, 1H)	52.10
5	8.319 (d, J=8.0 Hz, 1H)	
6		169.72
8	3.241 (m, 2H)	39.14
9	3.872 (bs, 1H)	52.38
10	7.8 to 8.6 (broad signal, 2H)	
11		169.95
13	1.875 (s, 3H)	22.52
14		170.04
16	8.422 (bd, J=7.1 Hz, 1H)	
17	4.259 (m, 1H)	48.69

Page X of X

NA = chemical shift assignment not available experimentally.
[a] position referring to structure in Figure 7.
[b] s = singlet; bs = broad singlet; d = doublet; bd = broad doublet, dd = doublet of doublets; ddd = doublet of doublet of doublets; t = triplet; m = multiplet
[c] δ_H referenced to CD_2HSOCD_3 at 2.50 ppm and δ_C referenced to DMSO-d_6 at 39.50 ppm.

2.4 Ultraviolet/Visible Spectrum

The Ultraviolet/Visible absorption spectrum of <INN> is presented in Figure 8. The spectrum was obtained using methanol as a solvent, recorded between XXX and XXX nm, with a scan rate of XX nm/min, and in a sample cell with a pathlength of 1 cm against a reference cell containing methanol. Absorption maxima are observed at XXX nm (ε: XXXXX.X $M^{-1}cm^{-1}$) and XXX nm (ε: XXXXX.X $M^{-1}cm^{-1}$).

Figure 8. UV/Visible Absorption Spectrum of <INN> Form X (Lot XXXXXXXXXX)

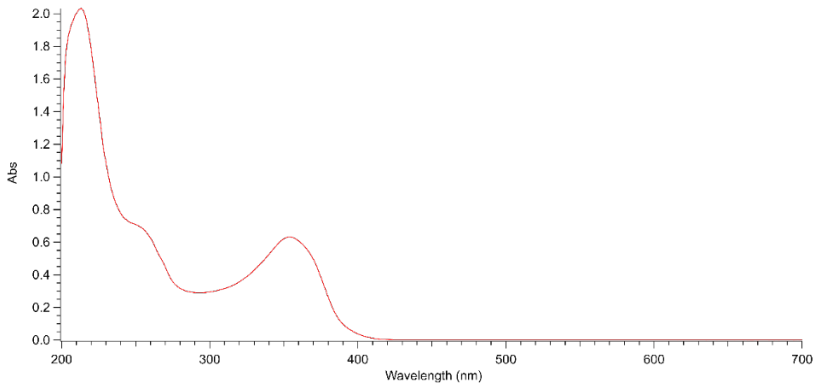

2.5 Infrared Spectrum

The infrared spectrum of <INN> was recorded between 4000 and 400 cm^{-1} on a Fourier Transform Infrared (FTIR) spectrophotometer with an Attenuated Total Reflectance (ATR) probe operating with resolution of 4.0 cm^{-1} and 32 scans (Figure 9). Assignments of the major bands observed in the spectrum were established in terms of the molecular structure of <INN> (Table 4). The absorption characteristics are consistent with the proposed structure.

Figure 9. Infrared Spectrum of <INN> Form X (Lot XXXXXXXXXX)

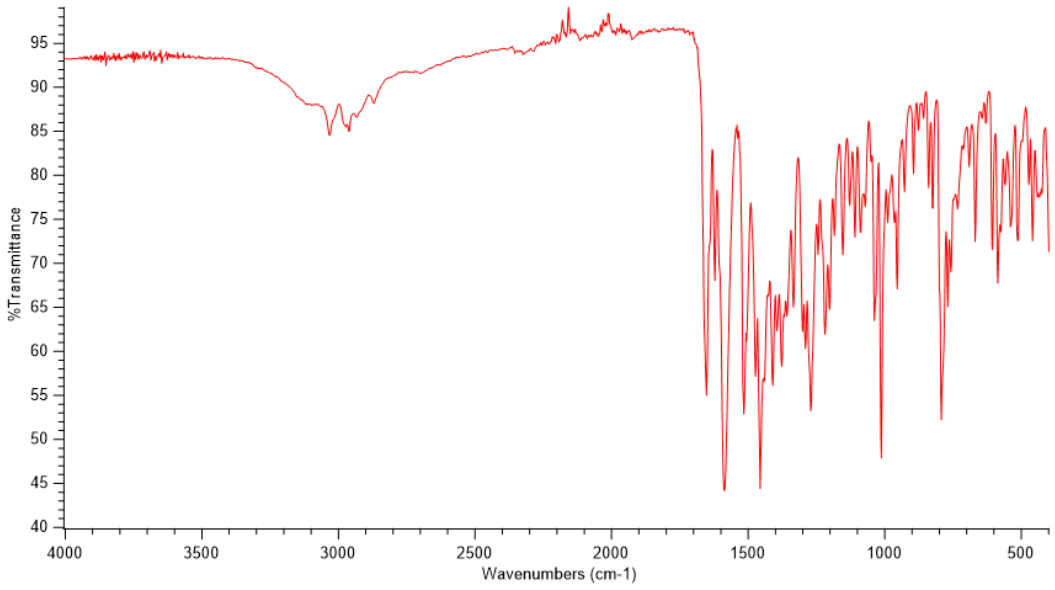

Table 4. Interpretation of the Infrared Spectrum of <INN>

Wavenumber (cm^{-1})	Relative Peak Intensity	Assignment
3100-3000	w	Aromatic C-H stretch
2975-2840	w	Aliphatic C-H stretch
1653	s	Tertiary Amide C=O stretch
1622	m	C=C conjugated with carbonyl stretch
1590-1575	s	Aromatic C=C stretch
1465-1440	s	CH_2, CH_3 bending
1270-1100	m-s	Aromatic Fluorine stretch
840-780	m	Aromatic C-H bending

s = strong, m = moderate, w = weak

2.6 Single Crystal X-ray Structure

Single crystals of <INN> Form X were utilized for X-ray diffraction study. X-ray data were collected using a charge coupled device-based diffractometer equipped with a

low-temperature apparatus operated at 173 K. The pertinent crystallographic parameters are summarized in Table 5. The single crystal structure shown in Figure 10 supports the proposed stereochemistry of <INN> in Section 2.7.

Table 5. Summary of Crystallographic Parameters for <INN> Form X (Lot XXXXXXXXX)

Wavelength	X.XXXX Å
Crystal System	Orthorhombic
Space Group	$P2_12_12_1$
Unit Cell Dimensions	a = XX.XXX Å α= 90° b = XX.XXX Å β= 90° c = XX.XXX Å γ = 90°
Volume	XXXX.X Å^3
Z	X
Z'	Y
Density (Calculated)	X.XXX g/cm^3
Absolute Structure Flack Parameter	X.XX(X)

Figure 10. Molecular Structure of <INN> in Form X (Lot XXXXXXXXX) Determined by Single Crystal X-ray Diffraction Analysis

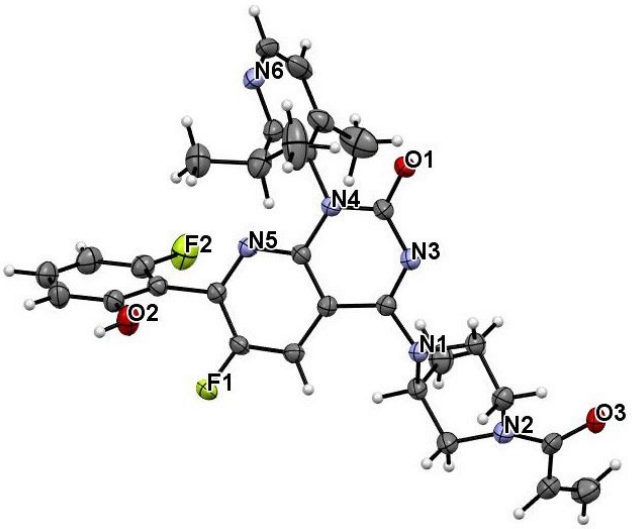

2.7 Isomerism

<INN> possess X stereocenters/asymmetric centers in <configuration>. When manufactured according to the process described in 3.2.S.2.2 (Description of Manufacturing Process and Process Controls), <INN> is obtained in high stereoisomeric

purity and has been found to be stable under the conditions of the synthesis. Chiral HPLC confirms that the desired <isomeric configuration> is stable with no conversion to <isomeric configuration> when held at XX°C for XX days.

2.8 Summary of Proof of Structure

Structural confirmation of <INN> has been established through <elemental analysis, mass spectrometry (MS), Single Crystal X-ray diffraction, and several spectroscopic techniques>.

^{1}H and ^{13}C NMR spectra confirm the number and character of the respective atoms; all chemical shifts correspond to expected values given the structure of <INN>.

IR spectroscopy confirms the presence of major functional groups present in the structure of <INN>.

Mass spectrometry confirms both the expected molecular mass and based on high resolution exact mass data, the molecular formula of <INN>. Fragment masses are consistent with expected fragmentation pattern.

Single Crystal X-ray diffraction confirms both the presence and arrangement of all heavy (ie, non-hydrogen) atoms in the molecule as well as the absolute configuration of the asymmetric center.

3. Physicochemical Characteristics

Physicochemical characterization of <INN> has been performed to evaluate <polymorphism, crystallinity, thermal properties, hygroscopicity, particle size distribution, pKa values and partition coefficient>. Details of the physicochemical characterization are provided in the sections below.

3.1 Polymorphism

Automated high throughput and manual polymorph screening experiments were conducted under various conditions to identify and characterize potential solid forms of <INN>. X crystalline forms, including X anhydrous forms, X amorphous forms and X solvate forms, have been discovered to date. These forms were characterized by <X-ray powder diffraction (XRPD), differential scanning calorimetry (DSC), thermogravimetric analysis (TGA) and dynamic vapor sorption (DVS)>. These techniques allowed identification and differentiation of all the solid state forms. Based on the comprehensive screening and characterization studies, anhydrous free base Form X was determined to be the most thermodynamically stable polymorph and was selected

for development. Form X is a crystalline, solvent-free form with low hygroscopicity (< X.X wt. % uptake at XX°C, XX% Relative Humidity (RH) and high melting point (XXX.X°C)).

<INN> drug substance manufacturing processes have consistently produced crystalline Form X as shown in Table 6.

Table 6. Summary of Solid State Properties for <INN> Form X GMP Lots

DS Lot Number (DS Manufacturing Process)	Form ID from XRPD	TGA Weight Loss up to 300°C	Melting Onset from DSC (°C)	Hygroscopicity from DVS (H_2O Uptake from 0 to 90% RH at RT)
XXXXXXXXXX (CP X.X)	Form X	0.1%	293.3	Not hygroscopic (0.5 wt.%)
XXXXXXXXXX (CP X.X)	Form X	0.3%	290.6	Not hygroscopic (0.4 wt.%)
XXXXXXXXXX (CP X.X)	Form X	0.2%	292.6	Not hygroscopic (0.2 wt.%)
XXXXXXXXXX (CP X.Y)	Form X	0.1%	288.9	Not hygroscopic (0.3 wt.%)
XXXXXXXXXX (CP Y.Y)	Form X	<0.1%	291.2	Not hygroscopic (0.3 wt.%)

The solid-state stability of Form X was monitored under various stressed conditions, as shown in Table 7. Form X was shown to be stable up to XX weeks under open container conditions of XX°C and XX% RH.

Table 7. Summary of Solid State Stability for <INN> Form X

Storage conditions	Time point	Form ID from XRPD	Melting onset from DSC (°C)	TGA weight loss (wt.%) from 25 to 300°C
Initial	0	Form X	286.8	0.03
40°C/75% RH (open)	2 weeks	Form X	286.1	0.06
	4 weeks		286.3	0.07
	14 weeks		285.3	0.04
25°C/60% RH (open)	2 weeks	Form X	285.3	0.07
	4 weeks		286.9	0.10
	14 weeks		286.0	0.09
60°C (open)	2 weeks	Form X	286.1	0.05
	4 weeks		286.1	0.07
	14 weeks		284.8	0.05
40°C (open)	2 weeks	Form X	285.7	0.04
	4 weeks		286.0	0.08
	14 weeks		285.1	0.08

The detailed solid state characterization studies showed that all solvate and hydrate forms convert to more stable Form X. From slurry conversion studies shown in Table 8, the thermodynamic stability of Form X was confirmed as the other anhydrous polymorphs Form Y and Form Z convert to Form X. Hydrated forms were also found to convert to Form X under various slurry conditions at room temperature.

Table 8. <INN> Form Conversion Study Summary

Initial Form	Conditions	Final Form
Amorphous Form	Slurry in water at room temperature for 48 hours	Anhydrous Free Form X
Mixture of Anhydrous Free Form X and Anhydrous Free Form Y	Water/acetonitrile (90/10) slurry at room temperature for 7 days	Anhydrous Free Form X
	Slurry in heptane at 80°C for 24 hours	
Anhydrous Free Form Y	Slurry in water at 90°C for 1 hour	Anhydrous Free Form X
	Heating at >250°C	
Mixture of Anhydrous Free Form X and Anhydrous Free Form Z	Slurry in ethanol at room temperature for 10 days	Anhydrous Free Form X
	Slurry in ethanol at 60°C for 5 days	
	Slurry in methanol at room temperature for 10 days	
Anhydrous Free Form Z	Slurry in water at room temperature and 60°C for 5 days	Anhydrous Free Form X
	Heating at 200-250°C	
Hydrate form	Slurry in methanol/water (75/25) at room temperature	Anhydrous Free Form X
	Slurry in ethanol/water (75/25) at room temperature	
	Slurry in NMP/water (2/98) at room temperature	
	Heating at 165°C followed by slurry in water at room temperature	

3.2 X-ray Powder Diffraction

The crystallinity and polymorph identity of <INN> were characterized using X-ray powder diffraction (XRPD) technique. Each sample was scanned between X and XX° in 2θ with a step size of X.XXXX° with CuKα wavelength of X.XX Å. The reference standard XRPD pattern of <INN> Form X is displayed in Figure 11. A list of the characteristic diffraction peak positions and relative intensities of Form X is given in Table 9.

Figure 11. X-ray Powder Diffractogram of <INN> Form X (Lot XXXXXXXXX)

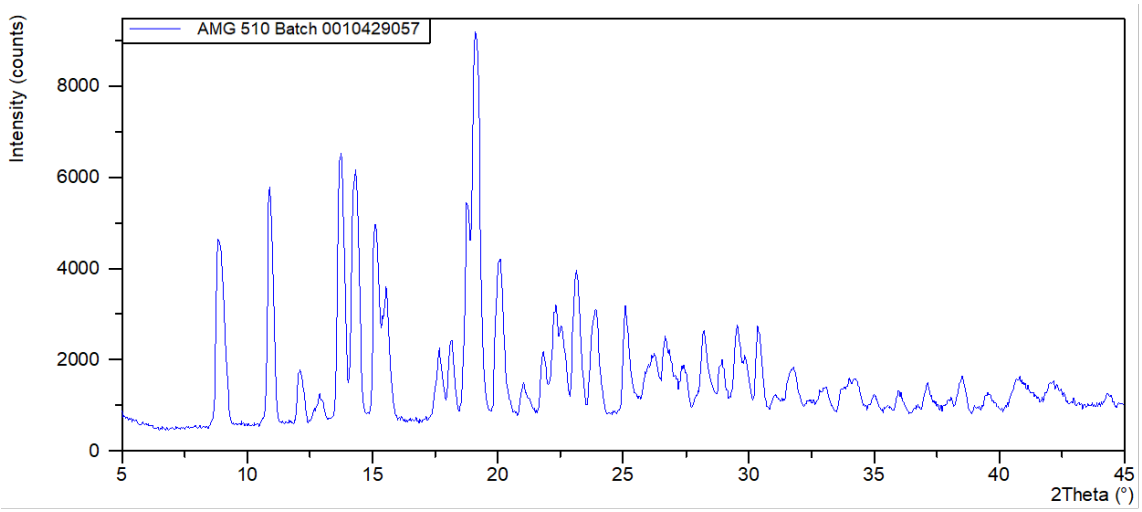

Table 9. List of Characteristic XRPD Peak Positions and Peak Intensities of <INN> Form X (Lot XXXXXXXXX)

Pos. [° 2θ]	Rel. Int. [%]
X.XX	XX.XX
XX.XX	XX.XX

3.3 Optical Rotation

The specific optical rotation of <INN> was determined to be +/-XX° using the analytical method described in 3.2.S.4.2 (Analytical Procedure).

3.4 Differential Scanning Calorimetry

The thermal transition characteristics of <INN> were determined using a differential scanning calorimetry (DSC) method. The measurement was performed under nitrogen gas flow with a heating rate of 10°C/min. The melting point of <INN> Form X was found to be XXX.X°C as an extrapolated onset.

Figure 12. DSC Thermogram of <INN> Form X (Lot XXXXXXXXX)

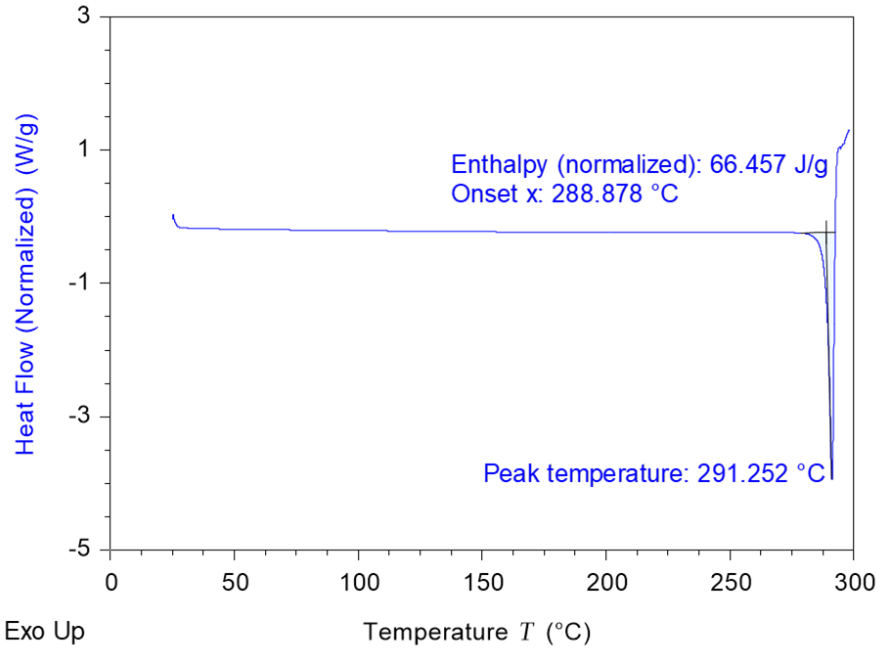

3.5 Thermogravimetric Analysis

Thermogravimetric analysis (TGA) of <INN> was performed under nitrogen gas flow at a heating rate of XX°C/min. A weight loss of X.XX% was observed from XX°C to XXX°C.

Figure 13. TGA Plot of <INN> Form X (Lot XXXXXXXXX)

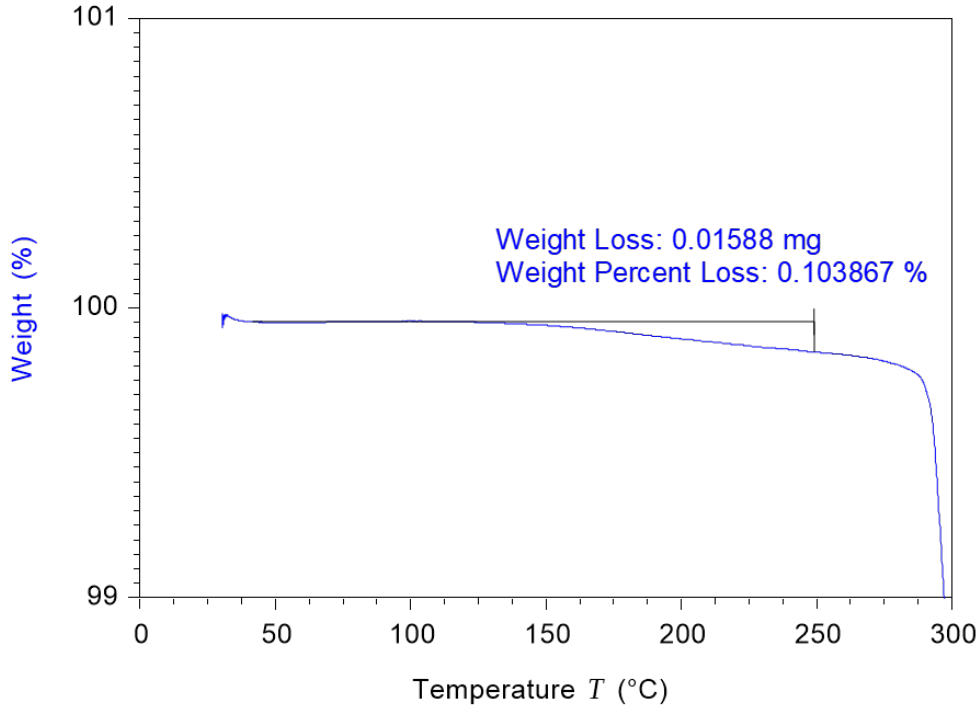

3.6 Hygroscopicity

The moisture uptake behavior of <INN> was evaluated using dynamic vapor sorption (DVS). The sample was placed into the DVS analyzer at 0% relative humidity (RH) at XX°C. The RH was increased from 0% to XX% in XX% increments and then decreased similarly back to 0% to complete a sorption/desorption cycle. The DVS isotherm plot shows moisture uptake of < X.X wt. % at XX% RH, indicating that <INN> Form X is slightly hygroscopic.

Figure 14. DVS Isotherm for <INN> Form X (Lot XXXXXXXXX)

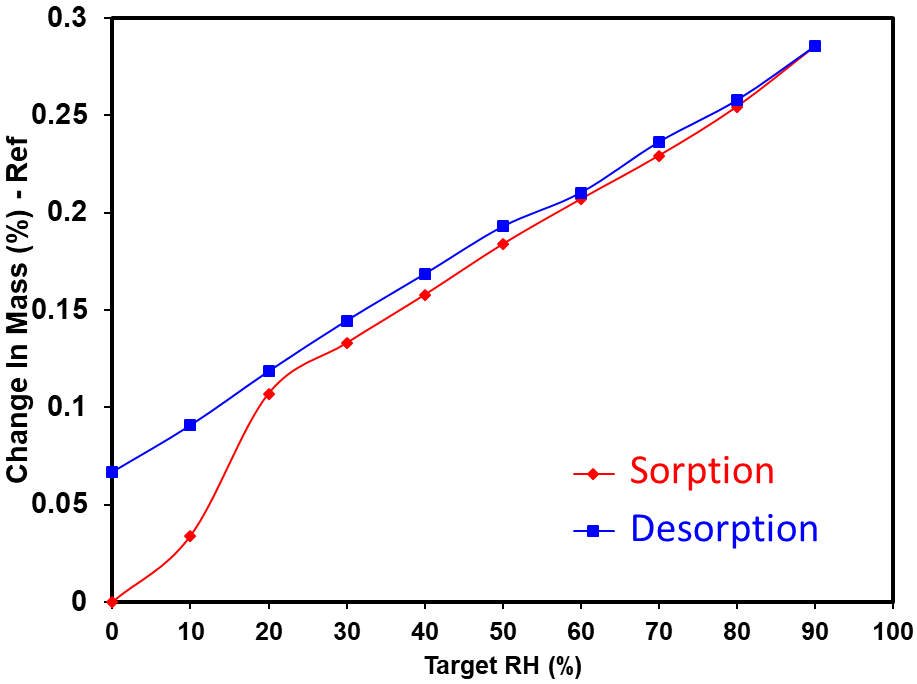

3.7 Particle Size Distribution

Particle size distribution (PSD) data for <INN> was collected using a laser light diffraction instrument, equipped with a liquid sample dispersion unit and optics suitable for detection of particle sizes between X.XX and XXXX μm. The PSD data of <INN> from several representative drug substance lots are summarized in Table 10.

Table 10. PSD Data for <INN> Form X

Lot	D_{10} (µm)	D_{50} (µm)	D_{90} (µm)
Development Lot (XXXXXXXXX)	X.X	XX.X	XX.X
Lead Lot (XXXXXXXXX)	X.X	XX.X	XX.X
Lot XXXXXXXXX (CP X.X)	X.X	XX.X	XX.X
Lot XXXXXXXXX (CP Y.X)	X.X	XX.X	XX.X

3.8 pKa Values

<INN> possesses two ionizing functional groups (amine and phenol) which may be titrated leading to dissociation constants.

The two pKa values were determined by 24-point parallel capillary electrophoresis with quantitation by UV absorbance at 228 nm. An aqueous solution of <INN> in acidic medium (10 mM HCl) was prepared at a concentration of 0.1 mg/mL. Capillary electrophoresis separations were carried out in parallel across 24 equally spaced pH values between X.X and XX.X. The compound migration time was monitored relative to a neutral marker (DMSO), and a titration curve was generated from this data.

The pKa values for <INN> were determined to be:

pKa_1 = X.XX (amine group)

pKa_2 = X.XX (phenol group)

3.9 pH of Aqueous Solution

A XX mg/mL suspension of <INN> was prepared in deionized (DI) water. After the suspension was agitated for XX hours at XX°C and excess solids were filtered, the aqueous solubility of <INN> was determined to be X.XXX mg/mL by HPLC analysis. The pH of aqueous solution was measured to be X.X.

3.10 Solubility Measurements

Solubility was determined by adding excess solute to various <buffer systems/solvents>. The resulting suspensions were agitated for XX hours at XX°C, followed by pH adjustment of the samples if required. The samples were then centrifuged, and supernatants were analyzed by a validated, stability indicating HPLC method. Solubility was measured in triplicate for all samples. Results are summarized in 3.2.S.1.3 (General Properties).

3.11 Partition/Distribution Coefficient

<<For non-ionizable molecules - Partition Coefficient (Log P)>>

The partition coefficient of <INN> was measured at XX°C using a shake flask method. The experimental partition was carried out using aqueous phases buffered with phosphate (Dulbecco's phosphate buffered saline (PBS) at pH = 7.4) and *n*-octanol saturated with buffered water. The flask was shaken to equilibrate the sample between the 2 phases, and the phases were then separated. Afterwards, the concentration of analyte was measured in both phases by RP-HPLC. The partition coefficient (Log P) of <INN> was measured to be X.XX

<<For ionizable molecules - Distribution Coefficient (Log D)>>

The distribution coefficient of <INN> was measured at XX °C using a shake flask method. The experimental partition was carried out using buffered aqueous phases with a pH of X.X, X.X, X.X, X.X and *n*-octanol saturated with buffered water. The flask was shaken to equilibrate the sample between the 2 phases, and the phases were then separated. Afterwards, the concentration of analyte was measured in both phases by RP-HPLC.

Table 11. Distribution Coefficient of <INN> as a Function of pH

pH	Distribution Coefficient (Log D)
X.X	X.XX
X.X	X.XX
X.X	X.XX
X.X	X.XX